

# IMPLEMENTATION AND EVALUATION OF A REACTION-DIFFUSION BASED CODING RATE CONTROL MECHANISM FOR CAMERA SENSOR NETWORKS

*Hiroshi Yamamoto, Katsuya Hyodo, Naoki Wakamiya, Masayuki Murata*

Graduate School of Information Science and Technology,  
Osaka University  
1-5 Yamadaoka, Suita, Osaka 565-0871, Japan

## ABSTRACT

Due to the limitation of wireless communication capacity, a camera sensor network will be easily congested and the perceived video quality considerably deteriorates, when all nodes generate and transmit high-quality video data. To tackle this problem, taking into account that not all video data are equally important from a viewpoint of surveillance or observation applications, our research group proposes an autonomous control mechanism, where each node appropriately determines its video coding rate according to the location and velocity of targets without any centralized control. In this paper, we implemented the mechanism and conducted practical experiments. We verified that the video coding rate was appropriately adjusted and the loss of packets was suppressed. Consequently, the perceived video quality was higher than the cases where the lowest coding rate was always used to avoid congestion and the highest coding rate was always used intending the high quality video.

**Index Terms**— Camera Sensor Network, Coding Rate Control, Reaction-Diffusion Model, Experiment

## 1. INTRODUCTION

By distributing a large number of sensor nodes with wireless communication capability and organizing a wireless sensor network (WSN), we can obtain detailed information about surroundings, remote region, and objects [1]. Sensor nodes are equipped with a variety of sensors depending on applications. In particular, a camera sensor network, which is composed of sensor nodes equipped with a camera, are useful in applications such as remote surveillance and monitoring [2] and thus it is one of key technologies for the safe and secure living environment. For example, by placing camera sensor nodes along streets, we can monitor the traffic condition, children on the way to and from a school, or track suspicious people.

Compared to typical sensor data such as humidity or temperature, the volume of video data generated by cameras are considerably large, ranging from a few hundred Kbps to several hundred Mbps. The capacity of wireless sensor networks

is limited to accommodate such huge video traffic. For example, the communication rate of ZigBee with IEEE 802.15.4 [3], a standard protocol for WSN, is only 250 Kbps. Even when we adopt IEEE 802.11b with the capacity of 11 Mbps, theoretical analysis indicates that the throughput available to each node is in the order of  $O(\frac{1}{\sqrt{n}})$ , where  $n$  is the number of nodes in the multi-hop wireless network [4]. Therefore, only a dozen of nodes can join the network, even when each node transmits video data coded at only a few Mbps using IEEE 802.11b. Many studies, such as bandwidth allocation, retransmission control [5], and FEC (Forward Error Correction) [6], have been made for QoS control for video transmission in wireless networks. They are useful and effective to maintain the quality of video data when a wireless network is lightly loaded and moderately congested, but they do not help much when the volume of video traffic is, for example, twice as much as the capacity of the network.

Therefore in large scale camera sensor networks, in addition to these QoS control mechanisms, application-level control to reduce the amount of video traffic without impairing the application is required. When we consider surveillance and monitoring applications, not all video data from cameras are equally important. Users are interested in video images that capture targets or certain phenomena. Therefore, the quality of video data from nodes detecting targets should be as high as possible without overwhelming the wireless network capacity, whereas those nodes far from the targets can suppress the video coding rate to avoid wasting the wireless network capacity by irrelevant and redundant video data. For this purpose, we need a mechanism for camera sensor nodes to adjust the video coding rate in accordance with the location and velocity of targets. To the best of our knowledge, such application-level control has not been addressed well and we can only find a few [7][8]. In [7], a content-aware control system assigning higher rate to cameras capturing important images is proposed. However, they mainly consider bandwidth allocation among cameras on a node, not among camera nodes. In [8], the authors propose dynamic allocation of wireless communication bandwidth to camera nodes based on the rate-distortion model and the activity of captured

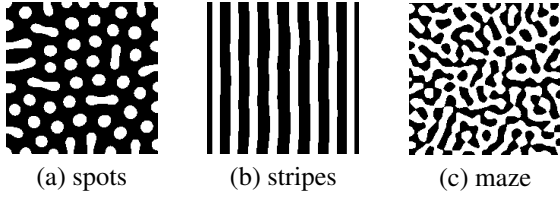


**Fig. 1.** Example of patterns generated by reaction-diffusion model

video. However, the bandwidth allocation is performed in a centralized manner, where a central location has the complete information about the status of wireless network and characteristics of video data at all cameras.

When we know the complete and up-to-date information about the location and status of camera sensor nodes and the location and velocity of targets, we can optimally assign the wireless network capacity to those nodes and set the video coding rate to avoid congestion of the network while keeping the application-level QoS. However, maintenance of such global and up-to-date information involves much communication overhead and the battery power of nodes. Therefore, an autonomous, distributed, and self-organizing mechanism is required for each node to appropriately determine the video coding rate based on local information obtained through message exchanging with neighboring nodes, while avoiding local network congestion.

Our research group proposed a reaction-diffusion based coding rate control mechanism to accomplish the goal without any centralized control [9]. A reaction-diffusion model is a mathematical model for pattern generation on the surface of body of mammals [10]. In a reaction-diffusion model, through local and mutual interaction among neighbor cells having two hypothetical morphogens, i.e. activator and inhibitor, a variety of heterogeneous spatial distribution of morphogen concentration emerges. In the proposed mechanism, we focus on the similarity between the coding rate distribution in a camera sensor network and a spot pattern generated in a self-organizing manner by a reaction-diffusion model. In a camera sensor network, the video coding rate is the highest at a node detecting a target in its observation area, nodes surrounding the node and those in the direction of target movement adopt the medium level of coding rate in preparing for future detection and detection error, and the others should keep the coding rate low. Consequently, we see spots centered at targets in the distribution of video coding rate in a camera sensor network. Similarly, the concentration of activator is the highest at the center of a spot in a reaction-diffusion pattern.

In our proposal, each node maintains the morphogen concentrations, which are periodically calculated based on the concentration information received from neighbor nodes. A node detecting a target sets the activator concentration high to generate a spot. Then, a node adjusts its coding rate based

on the derived concentration of morphogens. Through simulation experiments, we verified the effectiveness of our proposal in adjusting video coding rate according to the location and velocity of targets while keeping the total video traffic below the wireless network capacity. However, the simulation experiments were conducted assuming an ideal condition where there were no packet loss and no delay. In an actual situation, both of control packets and video data packets will be lost and it affects the perceived video quality.

In this paper, we implemented our reaction-diffusion based coding rate control mechanism on a wireless sensor network composed of PCs with camera and conducted practical experiments. We verified that the video coding rate was appropriately adjusted in accordance with the location and velocity of a moving target. We also evaluated the effectiveness of the mechanism in avoidance of congestion and the perceived quality of received video data.

The rest of paper is organized as follows. First in section 2, we introduce our reaction-diffusion based coding rate control mechanism for camera sensor networks. Next in section 3, we describe implementation of the mechanism. In section 4, we show results of experiments and discuss the effectiveness of the mechanism. Finally, we conclude the paper in Section 5.

## 2. REACTION-DIFFUSION BASED CODING RATE CONTROL MECHANISM FOR WIRELESS CAMERA SENSOR NETWORKS

Since the capacity of wireless networks is limited, we need a mechanism to control the amount of video traffic in a camera sensor network. In this section, we briefly describe our reaction-diffusion based mechanism for video coding rate control, where nodes autonomously adjust the video coding rate in accordance with the location and velocity of targets.

### 2.1. Reaction-Diffusion Model

A reaction-diffusion model was first proposed by Alan Turing as a mathematical model for pattern generation on the surface of body of mammals [10]. In a reaction-diffusion model, by mutual interaction among neighbor cells through chemical reaction and diffusion of two morphogens, spatially heterogeneous distribution of concentration of morphogens appears. Depending on the condition of a reaction-diffusion model, a variety of patterns as illustrated in Fig. 1 can be generated.

A reaction-diffusion model is formulated by a pair of partial differential equations.

$$\begin{aligned} \frac{\partial u}{\partial t} &= F(u, v) + D_u \nabla^2 u \\ \frac{\partial v}{\partial t} &= G(u, v) + D_v \nabla^2 v, \end{aligned} \quad (1)$$

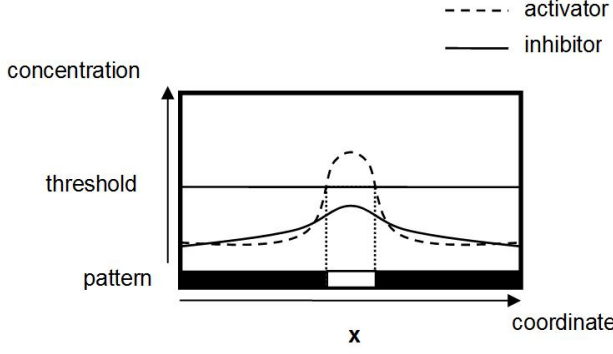


**Fig. 2.** Concentration distribution of activator and inhibitor

where  $u$  and  $v$  are the concentrations of activator and inhibitor, respectively.  $D_u$  and  $D_v$  are the diffusion rate of activator and inhibitor respectively.  $F$  and  $G$  are functions for reactions. The first term of the right-hand side is called a reaction term and the second term is called a diffusion term. In the reaction-diffusion model, the following two conditions must be satisfied to generate patterns. First, the activator activates itself and the inhibitor, whereas the inhibitor restrains itself and the activator. Second, the inhibitor diffuses faster than the activator ( $D_v > D_u$ ).

A mechanism of pattern generation can be explained as follows. In Fig. 2, those hypothetical chemicals are arranged in a line on the horizontal axis. The vertical axis corresponds to the concentrations of activator and inhibitor. Now consider that the concentration of activator has the peak at the point  $x$  illustrated in Fig. 2, by a slight perturbation. The concentrations of activator and inhibitor are increased around the point  $x$  by being activated by the activator. The generated inhibitor diffuses faster than the activator and restrains generation of activator at further regions. On the other hand, at the point  $x$ , because of the different rate of diffusion, the activator stays and the concentration of activator is kept higher than that of inhibitor. Consequently, the diversity in the concentration of activator emerges and a pattern appears. For example, when we color points where the concentration of activator exceeds a certain threshold with white and others with black, we can see a black-white-black pattern shown at the bottom of Fig. 2.

## 2.2. Reaction-Diffusion based coding rate control mechanism

Figure 3 illustrates a surveillance or monitoring system considered in [9]. Each square corresponds to the observation area of a camera sensor node. The darker the square is, the higher the coding rate is. In this system, nodes are arranged in a grid topology, considering town monitoring as an application of this mechanism. For example, we consider that camera sensor nodes are placed at intersections and they can

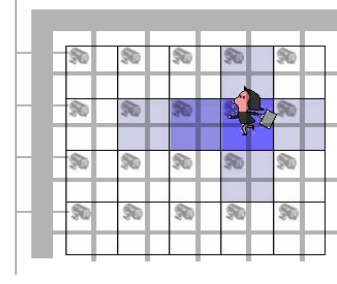


**Fig. 3.** Camera sensor network

communicate with four neighbors in up, right, down, and left directions.

A basic behavior of the reaction-diffusion based coding rate control mechanism is as follows. At regular control intervals, each node calculates the reaction-diffusion equation and derives the concentrations of activator and inhibitor by using the information which it received in the preceding control interval. When a node detects a target to monitor, it sets an increment of activator which is called *stimulus* in order to generate a spot centered at the node. Then it adjusts its coding rate in accordance with the derived morphogen concentrations. Finally, a node broadcasts a message containing information about its morphogen concentrations, stimulus, and the direction that the stimulus propagates. In [9], the following reaction-diffusion equation is used.

$$\begin{aligned} \frac{\partial u}{\partial t} &= F(u, v) + D_u \nabla^2 u + E(t) \\ \frac{\partial v}{\partial t} &= G(u, v) + D_v \nabla^2 v \end{aligned} \quad (2)$$

and

$$\begin{aligned} F(u, v) &= \max \{0, \min \{au - bv - c, M\}\} - du \\ G(u, v) &= \max \{0, \min \{eu - hv - f, N\}\} - gv, \end{aligned} \quad (3)$$

where  $a$  and  $e$  correspond to the rate of activation and  $b$  and  $h$  are for inhibition.  $c$  and  $f$  are parameters for decrease of morphogens per unit time.  $d$  and  $g$  are parameters for decomposition of morphogens per unit time.  $M$  and  $N$  are constants of limit.  $E(t)$  is the amount of stimulus at time  $t$ .

Since the arrangement of nodes and exchange of information are discrete in space and time, we discretize Eqs. (2) and (3) as follows.

$$\begin{aligned}
u_t &= u_{t-1} + \Delta t \left\{ F(u_{t-1}, v_{t-1}) - du_{t-1} + E(t-1) \right. \\
&\quad \left. + D_u \frac{(u_{t-1}^u + u_{t-1}^d + u_{t-1}^l + u_{t-1}^r - 4u_{t-1})}{\Delta h^2} \right\} \\
v_t &= v_{t-1} + \Delta t \left\{ G(u_{t-1}, v_{t-1}) - gv_{t-1} \right. \\
&\quad \left. + D_v \frac{(v_{t-1}^u + v_{t-1}^d + v_{t-1}^l + v_{t-1}^r - 4v_{t-1})}{\Delta h^2} \right\}
\end{aligned} \tag{4}$$

and

$$\begin{aligned}
F(u_{t-1}, v_{t-1}) &= \max \{0, \min \{au_{t-1} - bv_{t-1} - c, M\}\} \\
&\quad - du_{t-1} \\
G(u_{t-1}, v_{t-1}) &= \max \{0, \min \{eu_{t-1} - hv_{t-1} - f, N\}\} \\
&\quad - gv_{t-1}
\end{aligned} \tag{5}$$

At the  $t$ -th control timing, a node calculates the above reaction-diffusion equation to derive its morphogen concentrations  $u_t$  and  $v_t$ . A set of  $u_{t-1}^u, u_{t-1}^d, u_{t-1}^l, u_{t-1}^r$  and a set of  $v_{t-1}^u, v_{t-1}^d, v_{t-1}^l, v_{t-1}^r$  correspond to the concentration of activator and inhibitor of neighbor nodes in up, down, left, and right directions. These values are obtained from messages that a node received in the  $t-1$ -th control interval. The  $t-1$ -th control interval is defined as the duration from the  $t-1$ -th control timing to the  $t$ -th control timing. When a node did not receive a message from neighbor node in the  $t-1$ -th control interval, the latest value which was obtained before is used.  $\Delta t$  and  $\Delta h$  correspond to the discrete step interval of time and the distance between nodes, respectively.  $E(t-1)$  is the amount of stimulus which is determined at  $t$ -th control timing, based on messages which the node received in the  $t-1$ -th control interval and the condition of a target if exists.

A node which detects a target in the  $t-1$ -th interval sets the stimulus  $E$  and the attenuation  $A$  in accordance with the speed and direction of the target,  $E$  and  $A$  are appropriately chosen so that a spot pattern centered at the node is generated while keeping the total volume of traffic for the target lower than the wireless network capacity. For a fast-moving target, for example,  $A$  is set a larger value so that a spot spreads longer, but  $E$  becomes smaller not to increase the total volume. The determined  $E$  and  $A$  are embedded in a broadcast message together with the information indicating the direction of target movement, i.e. up, down, right, and left. A node which receives the stimulus information calculates its own stimulus  $E' = A \times E$ , if it is in the direction of diffusion of the stimulus, i.e. neighboring to the node detecting the target or in the direction of the target movement. Otherwise, it ignores this stimulus information.

Each node sets  $E(t-1)$  as the largest value of stimuli which are obtained from latest messages received from neighbor nodes. When a node detects a target by itself, it chooses a

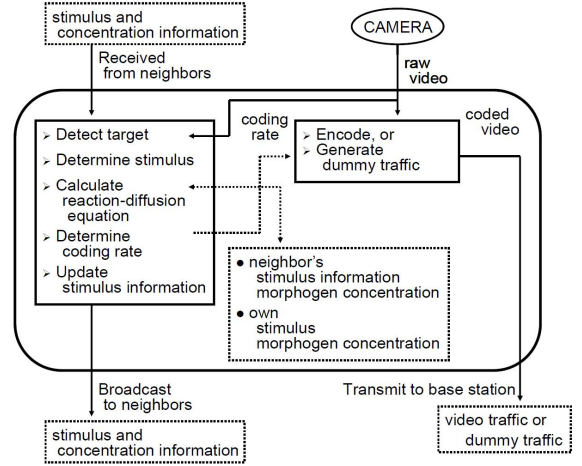


**Fig. 4.** Flow of information and data in a node

larger value among the  $E(t-1)$  and its own stimulus  $E$  as a new  $E(t-1)$ . Then, a node calculates the reaction-diffusion equation and determines its coding rate in accordance with  $u/\sqrt{v}$ . Finally, each node updates their stimulus information and broadcasts it.

When multiple targets are detected by nodes which are nearby, their patterns can be overlapped. In such a case, the activator concentration at the overlapped area unintentionally increases and the volume of generated traffic exceeds the wireless network capacity. To avoid this, in [9], a stimuli adjustment mechanism is proposed. When spot patterns are overlapped, a peak of inhibitor appears at the center of overlapped area. A node which detects a peak of inhibitor sets the NIP (Notification of Inhibitor Peak) flag in its broadcast message. The notification is forwarded to a source of the stimulus detecting a target by following the gradient of  $u/\sqrt{v}$  and the diffused stimulus. On receiving a message with NIP flag, a node detecting a target reduces the stimulus  $E$  as  $E \times \alpha$  ( $0 < \alpha < 1$ ). When targets move apart from each other and the overlap disappears, the stimulus has to be increased. A node which detects a target regularly increases the stimulus  $E$  as  $E + \Delta e$ , if it does not receive any NIP in the preceding control interval. To generate a pattern and not to flood the wireless network, there is the maximum and minimum values of stimulus.

In summary, with our mechanism, nodes can appropriately determine the video coding rate in accordance with location and velocity of targets through local interaction among nodes and without any centralized control. The quality of generated video data satisfies application requirements to observe targets clearly without overwhelming the wireless network capacity. We should note here that our mechanism assumes the fixed and stable wireless network capacity, since fluctuation in the capacity for instability of wireless communication links should be mitigated by underlying network and data link protocols.

speed (km/h)	$A$	maximum of $E$	minimum of $E$
$V = 0$	0.0	1960	830
$0 < V \leq 2$	0.2	1370	700
$2 < V \leq 4$	0.4	1010	440
$4 < V \leq 6$	0.6	620	390
$6 < V$	0.4	360	260

**Table 1.** Mapping from speed of target to stimulus and attenuation

$u/\sqrt{v}$	coding rate
$0 < u/\sqrt{v} \leq 5000$	0.75 Mbps
$5000 < u/\sqrt{v} \leq 10000$	1 Mbps
$10000 < u/\sqrt{v}$	2 Mbps

**Table 2.** Mapping from concentrations of morphogens to coding rate

### 3. IMPLEMENTATION OF THE REACTION-DIFFUSION BASED CODING RATE CONTROL MECHANISM

To verify our proposal in an actual environment, we implemented the mechanism and conducted experiments. In this section, we give an overview of our implemented system.

#### 3.1. Video Coding Rate Control

We used desktop or laptop PCs equipped with an IEEE 1394 camera and IEEE 802.11g wireless interface for a camera sensor node. Figure 4 shows how messages and video data are processed in a node. A node maintains information including the morphogen concentrations and stimuli on neighbor nodes and itself. At regular intervals, a node first checks whether it has a target in the observation area or not. If a target exists, a node determines the corresponding stimulus information, i.e.  $E$  and  $A$ , in accordance with the velocity of the target as in Table 1. Initially, the stimulus  $E$  is set at its maximum limit. These values are chosen assuming that the capacity of the wireless network consisting of four camera sensor nodes is 5 Mbps. Next, a node calculates the reaction-diffusion equation based on the morphogen concentrations of itself and neighbors and the stimuli. Then, it determines the coding rate based on the value  $u/\sqrt{v}$  as in Table 2. Finally, it broadcasts a message containing its morphogen concentrations, the stimuli information, and NIP, by using UDP/IP broadcasting. The payload size is 1649 bytes containing logging information.

By using the latest coding rate, a node generates MPEG-2 video data from raw video frames fed by a camera in YUV422 format. As an encoder, we used a software encoder called `mpeg2vidcodec_v12` developed by MSSG (MPEG Software Simulation Group) [11] and modified it so that the coding rate could be dynamically changed during coding a MPEG-2 stream. Video data are sent to a base station by using UDP/IP

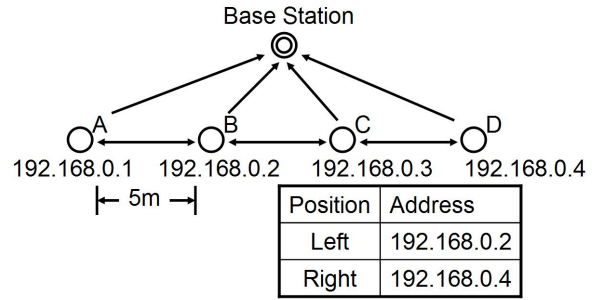


**Fig. 5.** Node layout in experimental system

unicast communication. The payload of one video data packet amounts to 1092 bytes.

#### 3.2. Object detection

Although some commercially available cameras are capable of object and motion detection, in our implementation, we used a simple mechanism for the purpose of preliminary experiments and easier control.

A node detects the existence and movement of an object by comparing the difference in luminance between two successive video frames. The luminance difference is derived for each pixel  $(i, j)$  by subtracting the luminance  $f(i, j)$  in the current frame from the luminance  $F(i, j)$  in the preceding frame. If the number of pixels whose absolute value of luminance difference is above the threshold  $x$  exceeds the threshold  $y$ , a node considers that there is a moving object in the observation area. The moving direction of the target is estimated by comparing the average coordinates of changed pixels in the successive several frames. Since estimation of the moving speed requires the complicated image processing such as estimation of the object size and its distance, we did not implement the speed detection mechanism and used the fixed value.

### 4. PRACTICAL EXPERIMENT AND RESULT

In this section, we show some results of our preliminary experiments to evaluate the effectiveness of our reaction-diffusion based video coding rate control.

#### 4.1. Experiment setting

In simulation experiments, we verified that each node could adjust their coding rate properly and the total amount of video traffic was suppressed by applying our proposal even for cases of multiple targets. However, due to time and facility limitation, the experiments in this paper were with only one target and four camera sensor nodes.

parameter	value	parameter	value
$a$	0.08	$h$	0.06
$b$	0.2	$D_u$	0.004
$c$	0.2	$D_v$	0.1
$d$	0.03	$M$	0.2
$e$	0.1	$N$	0.5
$f$	0.05	$\Delta t$	2.0
$g$	0.14	$\Delta h$	1.0

**Table 3.** Parameter setting

We arranged four camera sensor nodes 5 m apart in a line as illustrated in Fig. 5. A base station was located between nodes B and C and apart from the line. They were connected by IEEE 802.11 IBSS (Independent Basic Service Set) mode. All nodes belonged to the same IP subnet by having the same network address. Although all nodes were within the range of wireless communication, we manually configured them as a camera sensor node could exchange messages only with a base station and its both adjacent neighbors by using an address table. The control interval was set at 0.25 second. Thus, a node consumes 53 Kbps for control messages. All nodes operated asynchronously, where they broadcast messages, calculated the reaction-diffusion equation, and adjusted the coding rate at different timing. Other parameters used for the experiments are summarized in Table 3.

#### 4.2. Evaluation measures

We use packet loss rate and PSNR (Peak Signal to Noise Ratio) as measures of evaluation. The packet loss rate is defined as the ratio of the number of video data packets which are not received at a base station to the number of video data packets sent from camera sensor nodes. The PSNR is derived by the following equation.

$$PSNR = 20 \log_{10} \left( \frac{255}{\sqrt{MSE}} \right) \quad (6)$$

MSE represents the mean square error. MSE of an image of  $m \times n$  pixels is calculated the by following equation.

$$MSE = \frac{\sum (f(i, j) - F(i, j))^2}{mn} \quad (7)$$

where  $F(i, j)$  and  $f(i, j)$  are the luminance at the pixel  $(i, j)$  of an original image and that of a comparison image, respectively.

#### 4.3. Results and discussion

We first evaluated the performance of our implemented system and found that, to accomplish the detection, calculation, broadcasting, and coding in a real-time fashion, the spatial resolution and the frame rate should be kept as low as  $320 \times$

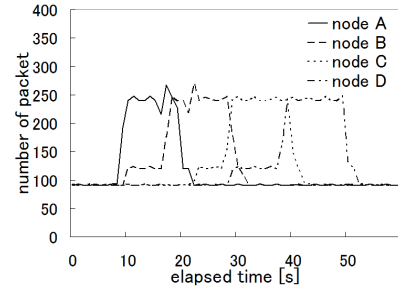


**Fig. 6.** the number of emitted packets with our proposal

240 pixels and 8 frames/sec, respectively. This results in the video rate of 1 Mbps at maximum and cannot cause congestion in the wireless network of only four nodes. Therefore, in the following, we use dummy traffic equivalent to video data of  $720 \times 480$  pixels and 30 frames/sec in size. On the base station, loss of video data packets was monitored and recorded, from which received video data were generated by using the video coding rate determined in experiments.

Figure 6 illustrates the time variation in the number of packets emitted by the camera sensor nodes per second when our proposal was applied. As the target walked at the speed of about 1.8 km/h from the left (node A) to the right (node D), it moved from the observation area of one node to another in about 10 seconds. This corresponds to the time variation in the video traffic shown in Fig. 6, where the duration that a node sent video data packets at the rate of about 250 packets/sec, i.e. 2 Mbps is about 10 seconds. A node in the direction of the target movement first raised its coding rate from 0.75 Mbps to 1 Mbps, and then set it at 2 Mbps on having the target in its observation area, and finally returned to its normal rate of 0.75 Mbps when the target disappeared from the observation area.

Next, in Fig. 7, we compare three alternatives focusing on the node C, which was located near the base station and thus affected by other traffic. As we do not see any visible gap between the number of packets sent by the node C and the number of packets received at the base station for the node C in Fig. 7 (a), the packet loss rate was only 0.01 % for the node C during the whole experiment. Figure 7 (b) shows the case of adopting the lowest coding rate, i.e. 0.75 Mbps, hesitating to generate the high quality video and introduce much video traffic into the network. In this case, the packet loss rate was the lowest and 0 %. Finally, the packet loss rate of the case where all nodes aggressively used the highest coding rate is shown in Fig. 7 (c). As shown in the figure, the considerable number of packets were lost and the loss rate was about 36.7 % for overloading the wireless network.

Figure 8 shows how the whole network was loaded. The figure illustrates the time variation in the total number of packets sent by all sensor nodes and the total number of packets the base station received. The number of received packets in

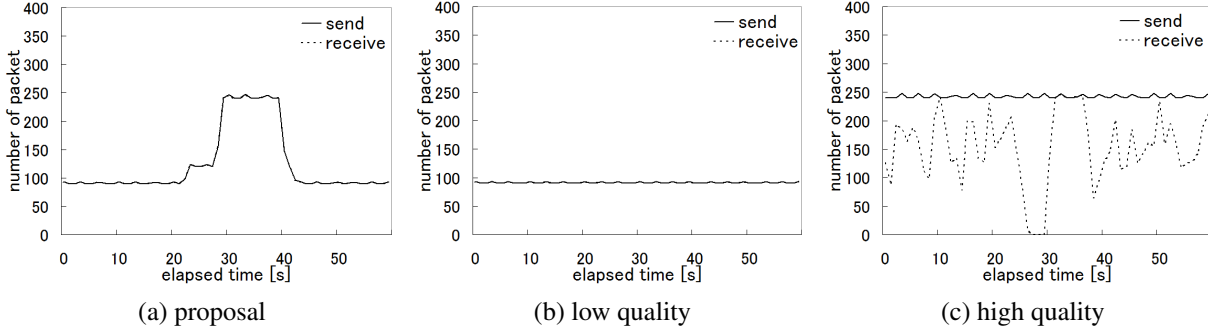


Fig. 7. the number of sent and received packets (Node C)

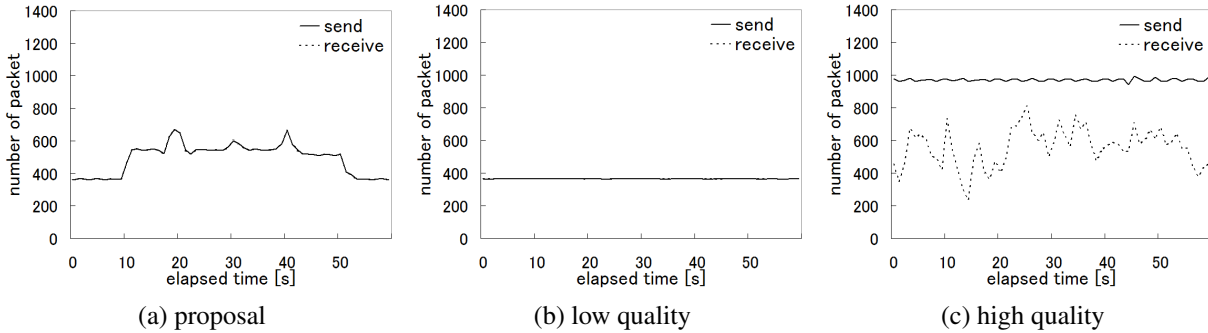


Fig. 8. the total number of sent and received packets

Fig. 8 (c) indicates the capacity of the wireless network. It is approximately 4.65 Mbps on average. It is almost equivalent to the total video traffic when one node uses the coding rate 2 Mbps, another node does that of 1 Mbps, and the other two nodes keep the lowest at 0.75 Mbps. In our proposal, the camera sensor nodes autonomously choose the optimal coding rate allocation in accordance with the location of the target by adopting the reaction-diffusion model. The average transmission rate of video data per node is about 1.03 Mbps with our proposal. The resultant packet loss rates are 0.24 %, 0.02 %, and 42.5 % in Figs. 8 (a), (b), and (c), respectively. The packet loss rates for nodes having the target in observation area are 0.03 %, 0 %, and 38.8 %, respectively.

The high packet loss rate severely affects the perceived video quality. Figure 9 shows the time variation in the PSNR value for video data sent by the node C and that received at the base station for the node C. The PSNR is derived against original video frames captured by a camera. Since the packet loss rate was too high to decode the received video data when the highest coding rate was always used, the PSNR values are only shown for the other two cases. In the case that our proposal was adopted, the node C adjusted the video coding rate in accordance with the target movement, as we see the increase in the PSNR to 40.0 dB at about 31 second. The reason for the instantaneous decrease of PSNR at about 29

second was for loss of packets containing the header information. This can be recovered by using FEC or we can avoid loss of header information by prioritizing important packets to the others. On the contrary, although such spike-like variation does not appear in Fig. 9 (b), the PSNR was around only 36.7 dB. Especially when the node C had the target in its observation area, the PSNR slightly decreased to 35.5 dB for the complexity and activity of captured images.

In conclusion, with our mechanism, camera sensor nodes autonomously adjusted video coding rate to avoid congestion of the wireless network in order to satisfy application requirements on the perceived video, where a user could monitor a target at the high quality description on a display.

## 5. CONCLUSION

In this paper, we implemented the reaction-diffusion based coding rate control mechanism on a camera sensor network and verified its effectiveness in an actual environment by practical experiments. We showed that network congestion was avoided and the quality of video data from a camera having a target was high.

Due to time and facility limitation, the experiments are preliminary with only four nodes and dummy traffic. We plan to conduct more realistic experiments where a camera

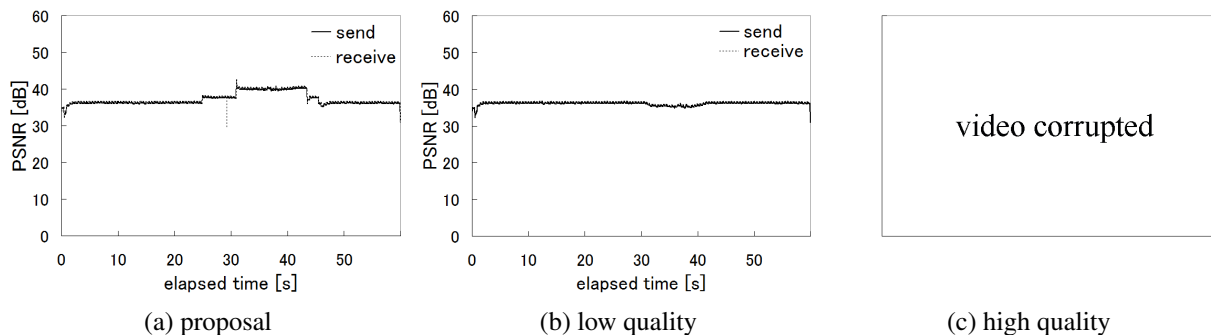


**Fig. 9.** PSNR of sent and received video data (Node C)

sensor network consists of dozens of camera sensor nodes, multiple targets exist, and video data are generated in a real-time fashion. Since nodes adopt multi-hop communication to send their video data to a base station in a large scale network, loss and delay of packets would occur more frequently and network-level control would influence on delivery of video data packets. We consider to adopt our reaction-diffusion based congestion control method where neighboring nodes interact with each other to balance the buffer occupancy on the whole network to mitigate network congestion [12]. We have already built a demonstration system for this and it works well. We also need to consider an algorithm to determine an appropriate set of parameters including  $E$ ,  $A$ , and the coding rate mapping.

#### ACKNOWLEDGEMENTS

This research was supported in part by “Special Coordination Funds for Promoting Science and Technology: Yuragi Project” of the Ministry of Education, Cululture, Sports, Science and Technology, Japan.

#### REFERENCES

- [1] I. F. Akyildiz, W. Su, Y. Sankarasubramaniam, and E. Cayirci, “Wireless sensor networks: a survey,” *Computer Networks*, vol. 38, no. 4, pp. 393–422, Mar. 2002.
- [2] I. F. Akyildiz, T. Melodia, and K. R. Chowdhury, “A survey on wireless multimedia sensor networks,” *Computer Networks*, vol. 51, no. 4, pp. 921–960, Mar. 2007.
- [3] ZigBee Alliance, “Zigbee specification,” June 2005, ZigBee Document 053474r06, Version 1.0.
- [4] Jinyang Li, Charles Blake, Douglas S.J. De Couto, Hu Imm Lee, and Robert Morris, “Capacity of ad hoc wireless networks,” in *Proceedings of the 7th Annual International Conference on Mobile Computing and Networking (MobiCom '01)*, Rome, Italy, July 2001, pp. 61–69.
- [5] Aura Ganz, Zvi Ganz, and Kitti Wongthavarawat, *Multimedia Wireless Networks: Technologies, Standards and QoS*, Springer, Sept. 2003.
- [6] Mark Watson, Michael Luby, and Lorenzo Vicisano, “Forward error correction (FEC) building block,” *Network Working Group RFC 5052*, Aug. 2007.
- [7] Ozturk, T. Hayashi, T. Yamasaki, and K. Aizawa, “Content-aware control for efficient video transmission of wireless multi-camera surveillance systems,” in *Proceedings of ACM/IEEE International Conference on Distributed Smart Cameras (ICDSC2007)*, Ph.D. Forum, Vienna, Austria, Sept. 2007, pp. 394–395.
- [8] X. Zhu, E. Setton, and B. Girod, “Rate allocation for multi-camera surveillance over an ad hoc wireless network,” in *Proceedings of Picture Coding Symposium (PCS-04)*, San Francisco, California, USA, Sept. 2004.
- [9] Katsuya Hyodo, Naoki Wakamiya, and Masayuki Murata, “Reaction-diffusion based autonomous control of camera sensor networks,” in *Proceedings of 2nd International Conference on Bio-Inspired Models of Network, Information, and Computing Systems (BIONET-ICS 2007)*, Dec. 2007.
- [10] A. M. Turing, “The chemical basis of morphogenesis,” *Royal Society of London Philosophical Transactions Series B*, vol. 237, pp. 37–72, Aug. 1952.
- [11] MSSG, “MPEG.ORG,” <http://www.mpeg.org/>.
- [12] A. Yoshida, T. Yamaguchi, N. Wakamiya, and M. Murata, “Proposal of reaction-diffusion based congestion control method for wireless mesh networks,” in *Proceedings of 10th International Conference on Advanced Communication Technology (ICACT 2008)*, Feb. 2008, pp. 455–460.